

This is the author-created version of the following work:

Tan, Sook Rei, Li, Changtai, and Yeap, Xiu Wei (2022) *A time-varying copula approach for constructing a daily financial systemic stress index*. North American Journal of Economics and Finance, 63 .

Access to this file is available from:

<https://researchonline.jcu.edu.au/76684/>

© 2022 Elsevier Inc. All rights reserved. AAM may be made open access in an Institutional Repository under a CC BY-NC-ND license after a 24 month embargo.

Please refer to the original source for the final version of this work:

<https://doi.org/10.1016/j.najef.2022.101821>

A time-varying copula approach for constructing a daily financial systemic stress index^{*}

Sook-Rei Tan^{a,*}, Changtai Li^b, Xiu Wei Yeap^c

^aJames Cook University Singapore, Business Department, 149 Sims Dr, Singapore 387380

^bPBC School of Finance, Tsinghua University, Beijing, China 100083

^cUniversiti Sains Malaysia, Economics Program, School of Social Sciences, Gelugor, Malaysia

Abstract

This paper develops a financial systemic stress index (FSSI) for the US financial market. We propose a time-varying copula method to model the dependence structure among financial sectors in order to build a correlated financial stress model that can signal systemic financial risks. The copula method is preferable to the traditional approach, enabling the modeling of non-linear correlations. Our analyses show that the dependencies across banking, security, and forex markets are best modeled by Archimedean copulas. Finally, we conduct a Markov Switching Autoregressive (MS-AR) model for FSSI and identify high financial stress episodes taking place in 2008-2009, 2011 and 2020.

Keywords: Financial stress index, copula, time-varying dependence, systemic stress, financial crisis

JEL Classification: C43, C58, G01, G10, G20

1. Introduction

Since the outbreak of the COVID-19 pandemic, global financial markets have been experiencing tremendous turmoil, which has manifested in volatile international capital movements and several stock market meltdowns of a scale and intensity comparable to those seen during the 2008 Global Financial Crisis (GFC). Fast forward to the present, wherein the financial markets appear to have returned to tranquility and the gradual reopening of the economy is anticipated, given widespread vaccine roll-outs around the world; all in all, future global economic prospects remain highly uncertain. This is further complicated by the recent spike in COVID-19 cases, which has impeded pace of reopening that may hamper economic recovery and investor confidence.

*This work was supported by the James Cook University Singapore Internal Research Grant (IRG20210009).

*Corresponding author

Email address: sookrei.tan@jcu.edu.au (Sook-Rei Tan)

Against the backdrop of elevated financial uncertainty induced by the ongoing COVID-19 crisis, this paper aims to introduce a copula-based daily financial systemic stress index (FSSI) that can be used, in time, to monitor the systemic financial stress of the US, taking into consideration time-varying dependence between different financial sectors. Our study is closely related to the strand of Financial Stress Index (FSI) literature pioneered by [Illing and Liu \(2006\)](#), who develop a continuous index of financial stress capable of measuring the intensity of crises for the Canadian financial system. In the aftermath of the GFC, the volume of FSI studies has grown substantially, and these studies can roughly be divided into two main branches based on their research objectives.

One branch of FSI literature focuses on applying FSI to explore the transmission of financial stress during crises. There are three main types of financial stress transmission studied in the extant literature: (1) Cross-market transmission – Such as [Chau and Deesomsak's \(2014\)](#) study, which examines FSI spillovers across the US equity, debt, banking, and forex markets and [Das et al.'s \(2018\)](#) article, which focuses on the relationships of gold, crude oil, and stocks with financial stress. (2) Cross-country transmission – For example, [Balakrishnan et al. \(2011\)](#) provided a seminal study on financial stress transmission from advanced economies to emerging economies; [Park and Mercado Jr \(2014\)](#) conducted a financial contagion analysis for 25 emerging market economies; [Apostolakis and Papadopoulos \(2014\)](#) studied financial stress spillovers across G7 economies; [MacDonald et al. \(2018\)](#) for the Eurozone; as well as [Elsayed and Yarovaya \(2019\)](#) for MENA countries. (3) Macro-finance transmission – See [Cardarelli et al. \(2011\)](#), who examined the relationship between FSI and the real economy for 17 advanced economies; and other similar studies such as [Hubrich and Tetlow \(2015\)](#) for the case of the US and [Aboura and van Roye \(2017\)](#) for the case of France.

The second branch of FSI literature focuses on refining the index, either by exploring the sets of components that should be embedded in the composite index to best represent the financial stress of a specific country (See for example, [Hakkio et al., 2009](#); [Nelson and Perli, 2007](#); [Oet et al., 2015](#); [Cevik et al., 2013](#); [Kliesen et al., 2010](#)), or explored the aggregation method for constructing the index. In line with the latter thread of research, [Hollo et al. \(2012\)](#) note the importance of capturing the systemic nature of financial crises by encapsulating the simultaneous correlations across financial sectors when constructing the stress indicator for the overall financial system. In building their Composite Indicator of Systemic Stress (CISS), the authors apply ideas from the portfolio theory approach, which weights the stress of each individual financial segment according to its time-varying cross-correlations with the other segments. In this manner, the CISS would put more weight on circumstances when high stress prevails in several financial markets

at the same time. This aggregation method has been adopted in other similar studies, including [Louzis and Vouldis \(2012\)](#) who developed an FSSI for Greece, and [Duprey et al. \(2017\)](#), who constructed a monthly Country-Level Index of Financial Stress (CLIFS) for the EU countries.

We follow the method of [Hollo et al. \(2012\)](#) to aggregate the stresses of banking, security, and forex markets into a single composite index using time-varying correlations between sectors as weights. However, unlike previous studies which use Pearson correlation coefficient that can only capture linear interrelationships between variables, we estimate a time-varying dependence structure across sectors using various types of copula functions, and use Kendall's Tau correlations from the best fitted copula as the subindices' weights.

A copula is a multivariate cumulative distribution function (CDF) formed by uniform marginal distributions of each random variable. The most noteworthy strength of the copula method lies in its flexibility and effectiveness in characterizing joint extreme movements between variables since this allows for the estimation of joint distribution through the separate assessment of the copula and the marginals. This motivates for the increased application of the copula method within the financial domain (such as, [Albulescu et al., 2020](#); [Aloui et al., 2013](#); [Bouri et al., 2018](#); [Zhang et al., 2018](#); [Nikoloulopoulos et al., 2012](#)) to deal with the asymmetric dependence of financial returns, a phenomenon in which the comovement of returns is stronger during crisis periods than non-crisis periods ([Patton, 2006](#)). With the presence of asymmetric comovements, traditional methods such as the Pearson correlation, which assumes a normal distribution and the linear dependency of different financial returns, may lead to an incorrect estimation of financial stress. As such, copula methods are used to overcome this limitation of traditional methods when the normality assumption is violated. By incorporating market specific weights with copula-based correlations, our FSSI can take into account possible nonlinear dependencies between the different financial segments of a system, thus more accurately reflecting the systemic behavior of financial stress.

The contributions of this paper are twofold. First, our paper adds to the evolving stream of financial stability literature by developing a copula-based FSI as a measure for financial instability. To our best knowledge, we are the first to apply the copula method in constructing a financial stress indicator. Second, investors and policymakers may use the FSSI as an indicator for financial risk. For example, financial regulators can employ the FSSI as a real-time warning signal for financial crisis, while investors may use the FSSI to aid their investment decisions and adjust their leverage dependent on the state of financial stress.

This paper is organized as follows: In Section 2, we introduce the market-specific stresses that constitute

the FSSI and provide a preliminary inspection of cross-market stress dependence, which motivates for the copula-based construction method of the FSSI. Section 3 explains the methodology of the copula models adopted in this paper and proposes an algorithm for deriving time-varying dependence measures. Section 4 presents the estimation results of the copula models. Section 5 aggregates the market-specific stresses into the FSSI and identifies systemic financial risk states. Section 6 provides a conclusion.

2. Constructing a copula-based FSSI

2.1. *Introducing components of market-specific stress*

The country-level FSSI comprises three stress subindices for banking, security, and forex markets, all of which are measured by real-time daily market-based indicators. The choice of indicators in this paper follows [Melvin and Taylor \(2009\)](#); [Cardarelli et al. \(2011\)](#); [Apostolakis and Papadopoulos \(2014\)](#). An overview of these subindices is provided as follows:

Banking market stress (I_{BK}). Stress in the banking market consists of three variables. First, in line with the standard capital asset pricing model, we measure the banking sector-specific shocks with the beta coefficient of the banking equity index, constructed as a 260-day rolling covariance of banking stock returns and the overall market returns relative to the variance of the overall market returns. Second, we include a TED or interbank spread, as given by the difference between 3-month interbank rates and yield on the Treasury Bill, to indicate the perceived credit risk in the banking sector. Third, the slope of the yield curve or inverted term spread, measured by the difference between the short- and long-term yields on government securities, is included to proxy a bank's profitability. Since a bank's profitability mainly hinges on its ability to convert short-term liabilities (demand deposits) into long-term assets (loans), a negative term spread poses a serious risk to the bank's income.

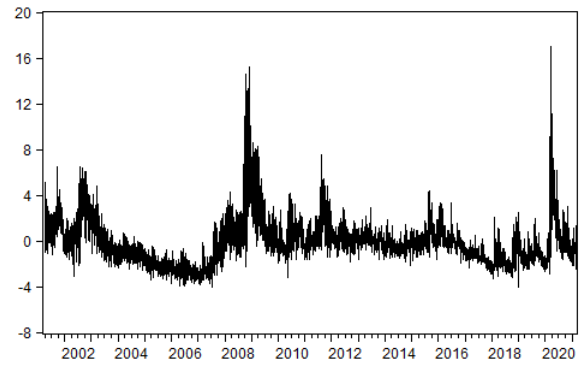
All the three indicators are standardized and averaged to obtain the banking market stress as :

$$I_{BK} = \frac{\text{beta} + \text{TED spread} + \text{Inverted term spread}}{3}$$

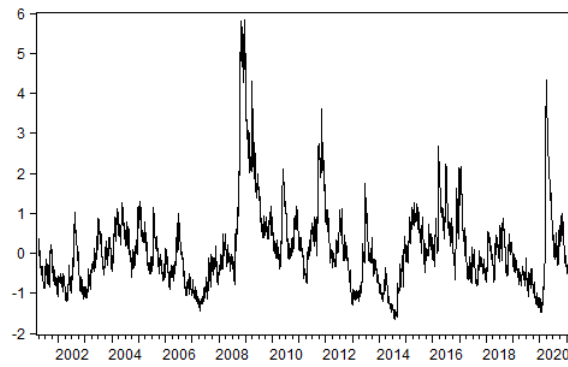
Security market stress (I_{SC}). Stress in the security market is constituted of three components. First, corporate bond spread as measured by the spread between yields on corporate bond and long-term government bond was used to proxy risk in the bond market. Second, we calculate inverted daily stock returns by multiplying -1 by the daily returns of S&P 500 composite index, such that a decline in stock returns is reflected as an increase in the security market stress. Third, we include the conditional stock market volatility



(a) banking



(b) security



(c) forex

Figure 1: Market-specific stress subindices

derived from an exponentially weighted moving average (EWMA)¹ of daily squared returns.

The security market stress is the average of the three standardized components as shown below:

$$I_{SC} = \frac{\text{Corporate bond spread} + \text{Stock returns} + \text{Stock volatility}}{3}$$

Forex market stress (I_{FX}) . Stress in the forex market is indicated by the time-varying volatility of forex returns, as proxied by standardized EWMA volatility of daily changes of nominal effective exchange rates.

$$I_{FX} = \text{Forex volatility}$$

Table 1: Descriptive Statistics

	Bank	Security	Forex
Mean	-0.0006	-0.0379	0.1005
Maximum	2.9356	17.0249	5.8240
Minimum	-1.1725	-4.0928	-1.6411
Std. Dev.	0.5504	2.0706	1.0262
Skewness	0.4222	1.9181	1.9486
Kurtosis	3.8643	10.4288	9.2145
Jarque-Bera	316***	15149***	11661***
ARCH test (5)	47460***	1089***	36465***
Ljung-Box test (5)	25657***	15108***	24597***
Observations	5201	5201	5201

Notes: *, **, and *** denote significance at the 10, 5 and 1% level.

2.2. A preliminary analysis of market-specific stresses

Using daily market data from the US that span the period from March 30, 2001, to March 5, 2021, we construct the stress placed on banking, security, and forex markets as plotted in [Figure 1](#). We observe that heightened stress occurred in the GFC period across all three markets. Specifically, the stress on both the banking and forex markets peaked at 2008, with a more abrupt pattern seen in the forex stress. During early 2020, when the COVID-19 pandemic first emerged, all three markets were hit by stress on a scale comparable to the GFC period. Most strikingly, the security market stress during the COVID-19 period surpassed that of the GFC period albeit a milder surge was found in the stress experienced by the banking and forex markets.

[Table 1](#) presents the descriptive statistics of the three market-specific stresses. Both banking and security stresses have negative means, while forex stress has a positive mean. All three subindices are skewed to the right. The kurtosis of all market stresses exceeds three, indicating the presence of a heavy-tailed distribution for all three series. The non-zero skewness and excess kurtosis suggest that the financial stress is not normally distributed, a result further substantiated by the Jarque-Bera test. The significant ARCH test and Ljung-Box test confirm the existence of the ARCH effect and autocorrelation.

As a preliminary examination of the cross-market dependence structure, we adopt a graphical tool known as a Chi-plot, developed by [Fisher and Switzer \(1985, 2001\)](#). The Chi-plot inspects the dependency pattern

¹A 60-day rolling window is adopted, and the decay factor λ is set as 0.94 following the parameter setting stipulated by the JP Morgan RiskMetrics database.

between two series by comparing the empirical bivariate distribution against the null hypothesis of independence at each point in the scatter plot. Specifically, the bivariate distribution H and the two marginal distributions F and G of the two series (\mathbf{x}, \mathbf{y}) can be calculated using a nonparametric method as follows:

$$H_i = \frac{1}{n-1} \sum_{j \neq i} I(x_j \leq x_i, y_j \leq y_i),$$

$$F_i = \frac{1}{n-1} \sum_{j \neq i} I(x_j \leq x_i),$$

$$G_i = \frac{1}{n-1} \sum_{j \neq i} I(y_j \leq y_i).$$

where $I(A) = 0, 1$ according to whether A is false or true.

Then, the Chi-plot is generated by creating a scatter plot for each pair of indices (λ_i, χ_i) based on:

$$\chi_i = \frac{H_i - F_i G_i}{\sqrt{F_i(1-F_i)G_i(1-G_i)}}$$

and

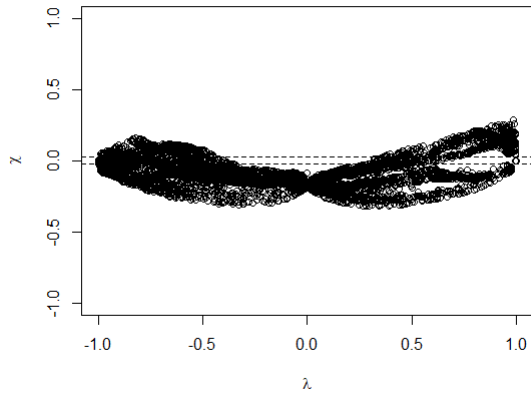
$$\lambda_i = 4 \operatorname{sign}(\tilde{F}_i \tilde{G}_i) \max(\tilde{F}_i^2, \tilde{G}_i^2)$$

where $\tilde{F}_i = F_i - \frac{1}{2}$, $\tilde{G}_i = G_i - \frac{1}{2}$ for $i \in \{1, \dots, n\}$. To eliminate outliers, only the points that satisfy $|\lambda_i| < 4\{\frac{1}{n-1} - \frac{1}{2}\}^2$ are included in the display.

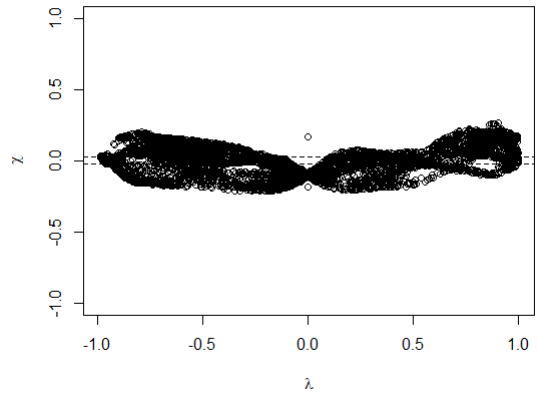
The parameter λ_i is a measure of the distance of the sample point (x_i, y_i) from the center of the dataset, and the value of χ_i is a measure of the distance of the joint distribution H to the distribution of independent pairs of random variables (\mathbf{x}, \mathbf{y}) . Since $H_i = F_i G_i$ for all i under independence, values of χ_i that situate far from zero (beyond the 95 percent confidence band) imply a departure from independence.

Figure 2 illustrates Chi-plots for each pair of market stresses. All pairs of subindices exhibit heavy-tail dependence, given that most distribution points fall outside the confidence bands with obvious curvature. Specifically, the dependencies are negative between the banking and security markets, and between the banking and forex markets. Meanwhile, positive dependence is found between the security and forex markets.

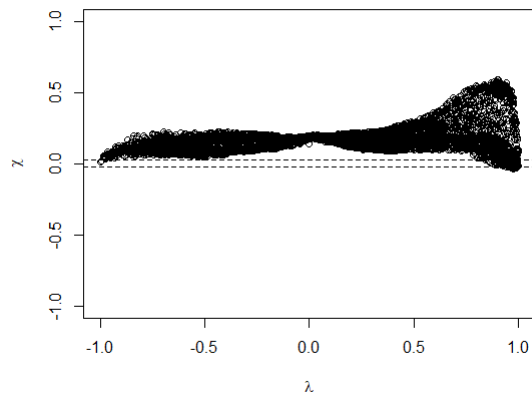
The Chi-plots provide a preliminary analysis of nonlinear dependence structures across market stresses and motivate for the use of the copula method to model such nonlinear dependencies.



(a) banking-security



(b) banking-forex



(c) security-forex

Figure 2: Chi-plots illustrated by each pair of subindices

2.3. A portfolio based aggregation approach to FSSI construction

Following the portfolio theory approach adopted by [Hollo et al. \(2012\)](#), the three market subindices are aggregated to a single composite indicator of system risk, namely, an FSSI, by weighting each component according to the pairwise cross-market correlations. In this setting, the overall financial stress would be intensified in the face of increased market co-movements. In contrast, lower cross-market linkages would mitigate any diversifiable risk, resulting in a lower risk of overall financial stress.

The three-market FSSI is computed as:

$$FSSI_t = \mathbf{I}_t \cdot C_t \cdot \mathbf{I}_t' \quad (1)$$

where $\mathbf{I}_t = (I_{BK}, I_{SC}, I_{FX})$ and C_t is the matrix of the time-varying cross-correlations of the subindices:

$$C_t = \begin{bmatrix} 1 & \tau_{BK,SC,t} & \tau_{BK,FX,t} \\ \tau_{BK,SC,t} & 1 & \tau_{SC,FX,t} \\ \tau_{BK,FX,t} & \tau_{SC,FX,t} & 1 \end{bmatrix}$$

The cross correlations $\tau_{i,j,t}$ are Kendall's Tau coefficient, a measure of rank correlation, corresponding to the best fitted time-varying copula estimated in the next section.

3. Copula Methodology

To model and analyze the dependence structure among the banking, security, and forex sectors, we employ a copula analysis.

Copula methods are widely used to measure the dependence structures (joint distribution) of two or more variables. This is based on the [Sklar's theorem \(1959\)](#), which states that a multivariate distribution can be expressed in terms of univariate marginal distribution functions and a copula function. By estimating the marginals and copulas separately, one can relax the assumptions of normality and linear correlation when constructing the multivariate distribution. In addition, the left and right tail dependencies can be measured using asymmetric copula families, such as the Archimedean copula, circumventing the assumption of symmetric tail dependence that goes with a normal distribution function.

An n-dimensional copula $c(\mu_1, \mu_2, \dots, \mu_n)$ is defined as a distribution function on $I^n = [0, 1]^n$ with standard uniform marginal distributions ([Tsay, 2013](#)). According to Sklar's theorem, every n-dimensional distribution

of a random vector, $X = (x_1, x_2, \dots, x_n)$ with marginals $F_1(x_1), F_2(x_2), \dots, F_n(x_n)$ can be written as follows:

$$F(x_1, x_2, \dots, x_n) = C(F_1(x_1), F_2(x_2), \dots, F_n(x_n)),$$

where C is a copula that is uniquely determined on I^n for the distribution F with absolutely continuous margins as:

$$C(\mu_1, \mu_2, \dots, \mu_n) = F(F_1^{-1}(\mu_1), F_2^{-1}(\mu_2), \dots, F_n^{-1}(\mu_n)).$$

There are various families of copulas in the existing literature, including elliptical, Archimedean, Fréchet, Farlie–Gumbel–Morgenstern, Extreme Value, Asymmetric Logistic Model, and the Convex Combinations copulas. Among these copula families, the elliptical and Archimedean copulas are the two most widely used copulas in finance and economic application (Yeap et al., 2020). In this paper, we focus on the Gaussian and Student's t copulas from the elliptical family, as well as Frank, Clayton, Gumbel, and Joe copulas from the Archimedean family. The Gaussian distribution is a widespread distribution in financial modeling, while the Student's t distribution is used to model extreme symmetric tail dependence. The four copulas chosen from the Archimedean family are also commonly used in financial engineering due to their various unique features. Specifically, the Frank copula is able to describe tail independence, while the Clayton, Gumbel, and Joe copulas are able to capture asymmetric dependence structures.

In the following, we present the functional forms of the selected copulas as mentioned above.

(i) The Gaussian copula. In n -dimension, the Gaussian copula can be expressed as:

$$C(\mu_1, \mu_2, \dots, \mu_n; \Sigma) = \Phi_n\left(\Phi^{-1}(\mu_1), \Phi^{-1}(\mu_2), \dots, \Phi^{-1}(\mu_n)\right) \quad (2)$$

where Φ_n and Φ^{-1} are the standard multivariate Gaussian and the inverse of the standard univariate Gaussian. Σ is the linear correlation matrix for the multivariate normal distribution. From Equation 2, the bivariate copula and its density can be expressed as:

$$C(\mu_1, \mu_2; \rho) = \Phi_2\left(\Phi^{-1}(\mu_1), \Phi^{-1}(\mu_2); \rho\right)$$

$$c(\mu_1, \mu_2; \rho) = \frac{1}{\sqrt{1-\rho^2}} \exp\left(-\frac{1}{2(1-\rho^2)}(x_1^2 - 2\rho x_1 x_2 + x_2^2)\right)$$

where x_1 and x_2 are random variables and ρ is their linear correlation coefficient. For $\rho = 1$ and $\rho = -1$, the copulas are comonotonic and counter-monotonic, respectively. For $\rho = 0$, the copula is independent.

Tail dependence is the measurement of dependence at the extreme quantiles. Upper tail dependence λ_U

and lower tail dependence λ_L are defined as follows:

$$\lambda_U = \lim_{\zeta \rightarrow 1^-} P\{\mu_1 > F_1^{-1}(\zeta) \mid \mu_2 > F_2^{-1}(\zeta)\} = \lim_{\zeta \rightarrow 1^-} \frac{1 - 2\zeta + C(\zeta, \zeta)}{1 - \zeta}$$

$$\lambda_L = \lim_{\zeta \rightarrow 0^+} P\{\mu_1 \leq F_1^{-1}(\zeta) \mid \mu_2 \leq F_2^{-1}(\zeta)\} = \lim_{\zeta \rightarrow 0^+} \frac{C(\zeta, \zeta)}{\zeta}$$

where $F_1^{-1}(\zeta)$ and $F_2^{-1}(\zeta)$ are the marginal quantile functions of the two variables μ_1 and μ_2 at the level ζ . Since the Gaussian copula exhibits no asymmetric behavior, both lower and upper tail dependencies are equal to zero ($\lambda_L = \lambda_U = 0$).

(ii) The Student's t copula. In n-dimension, the Student's t copula can be expressed as:

$$C(\mu_1, \mu_2, \dots, \mu_n; \Sigma, \nu) = T_\nu \left(t_{\nu_1}^{-1}(\mu_1), t_{\nu_2}^{-1}(\mu_2), \dots, t_{\nu_n}^{-1}(\mu_n) \right) \quad (3)$$

where T_ν and $t_{\nu_1}^{-1}$ are the standard multivariate Student's t and the inverse of the standard univariate Student's t with ν and ν_1 degrees of freedom, respectively. Σ is the linear correlation matrix for the multivariate Student's t distribution. From Equation 3, the bivariate Student's t copula and its density can be expressed as:

$$C(\mu_1, \mu_2; \rho, \nu) = T_\nu \left(t_{\nu_1}^{-1}(\mu_1), t_{\nu_2}^{-1}(\mu_2); \rho, \nu \right)$$

$$c(\mu_1, \mu_2; \rho, \nu) = \frac{K}{\sqrt{1 - \rho^2}} \left(1 + \frac{1}{V(1 - \rho^2)} (\xi_1^2 - 2\rho\xi_1\xi_2 + \xi_2^2) \right)^{\frac{\nu+2}{2}} \left[(1 + \nu^{-1}\xi_1^2)(1 + \nu^{-1}\xi_2^2) \right]^{\frac{\nu+2}{2}}$$

where $\xi_i = t_{\nu_i}^{-1}(\mu_i)$ and $K = \Gamma\left(\frac{\nu}{2}\right)\Gamma\left(\frac{\nu+1}{2}\right)^{-2}\Gamma\left(\frac{\nu}{2} + 1\right)$. ρ is the linear correlation coefficient of the bivariate Student's t distribution with ν degree of freedom. The Student's t copula is symmetric in tail dependence, and it approximates the Gaussian copula when the degree of freedom is large. The coefficient of tail dependence can be expressed as:

$$\lambda_L = \lambda_U = 2t_{\nu+1} \left(\frac{\sqrt{\nu+1}\sqrt{1-\rho}}{\sqrt{1+\rho}} \right)$$

(iii) The Frank copula. In n-dimension, the Frank copula can be expressed as:

$$C(\mu_1, \mu_2, \dots, \mu_n; \theta) = -\frac{1}{\theta} \ln \left(1 + \frac{\sum_{i=1}^n \exp(-\theta\mu_i) - 1}{\exp(-\theta) - 1} \right) \quad (4)$$

where θ is the copula parameter that takes any real value from $-\infty$ to ∞ . This copula can capture both positive and negative dependence of the random variables. The copula is independent when $\theta = 0$, comonotonic when θ approaches ∞ , and counter-monotonic when θ approaches $-\infty$. From Equation 4, the bivariate Frank

copula and its density can be expressed as:

$$C(\mu_1, \mu_2; \theta) = -\frac{1}{\theta} \ln \left(1 + \frac{(\exp(-\theta\mu_1) - 1)(\exp(-\theta\mu_2) - 1)}{\exp(-\theta) - 1} \right)$$

$$c(\mu_1, \mu_2; \theta) = \frac{\theta[1 - \exp(-\theta)] \exp(-\theta u_1 u_2)}{([1 - \exp(-\theta)] - (1 - \exp(-\theta u_1))(1 - \exp(-\theta u_2)))^2}$$

The Frank copula does not have lower and upper tail dependence ($\lambda_L = \lambda_U = 0$) like the Gaussian copula. This copula is more suitable for capturing the dependency of variables that are weak in tail dependence.

(iv) The Gumbel copula. In n-dimension, the Gumbel copula can be expressed as:

$$C(\mu_1, \mu_2, \dots, \mu_n; \delta) = \exp \left(- \sum_{i=1}^n (-\ln(u_i))^\delta \right)^{1/\delta} \quad (5)$$

The Gumbel copula parameter takes values from range of one to infinity and it can only capture positive dependence. The copula is independent when $\delta = 1$ and comonotonic when $\delta \rightarrow \infty$. From Equation 5, the bivariate Gumbel copula and its density can be expressed as:

$$C(\mu_1, \mu_2; \delta) = \exp \left\{ - \left([-\ln(\mu_1)]^{1/\delta} + [-\ln(\mu_2)]^{1/\delta} \right)^\delta \right\}$$

$$c(\mu_1, \mu_2; \delta) = (A + \delta - 1) A^{1-\delta} \exp(-A) (u_1 u_2)^{-1} (-\ln u_1)^{\delta-1} (-\ln u_2)^{\delta-1}$$

where $A = [(-\ln(\mu_1))^\delta + (-\ln(\mu_2))^\delta]^{1/\delta}$. As the Gumbel copula is an asymmetric copula that can only capture the upper heavy tail, there is no lower tail for the Gumbel copula ($\lambda_L = 0$). The upper tail is $\lambda_U = 2 - 2^{1/\delta}$ for all δ larger or equal to one.

(v) The Clayton copula. In n-dimension, the Clayton copula can be expressed as:

$$C(\mu_1, \mu_2, \dots, \mu_n; \alpha) = \left(- \sum_{i=1}^n u_i^{-\alpha} - n + 1 \right)^{\frac{1}{\alpha}} \quad (6)$$

where α is the Clayton parameter from the range of zero to infinity and n is the number of random variables. The copula is independent when $\alpha \rightarrow 0$ and comonotonic when $\alpha \rightarrow \infty$. From Equation 6, the bivariate Clayton copula and its density can be expressed as:

$$C(\mu_1, \mu_2; \alpha) = (u_1^\alpha + u_2^\alpha - 1)^{\frac{1}{\alpha}}$$

$$c(\mu_1, \mu_2; \alpha) = (1 + \alpha) \left(u_1^{-\alpha} + u_2^{-\alpha} - 1 \right)^{-\frac{1}{\alpha}-2} (u_1 u_2)^{\alpha-1}$$

As the Clayton copula is an asymmetric copula that can only capture the lower heavy tail, there is no upper

tail for the Clayton copula ($\lambda_U = 0$). The lower tail is $\lambda_L = 2^{-1/\alpha}$ for all α larger than zero.

(vi) The Joe copula. In n-dimension, the Joe copula can be expressed as:

$$C(\mu_1, \mu_2, \dots, \mu_n; \beta) = 1 - \left(1 - \prod_{i=1}^n (1 - (1 - \mu_i)^\beta) \right)^{1/\beta} \quad (7)$$

where β is the Joe parameter from the range of one to infinity. The copula is independent when $\beta \rightarrow 1$ and comonotonic when $\beta \rightarrow \infty$. From Equation 7, the bivariate Joe copula and its density can be expressed as:

$$C(\mu_1, \mu_2; \beta) = 1 - \left[(1 - \mu_1)^\beta + (1 - \mu_2)^\beta - (1 - \mu_1)^\beta (1 - \mu_2)^\beta \right]^{1/\beta}$$

$$c(\mu_1, \mu_2; \beta) = \frac{\left((1 - (1 - \mu_1)^\beta)(1 - \mu_2)^\beta + (1 - \mu_1)^\beta \right)^{\frac{1}{\beta}} \left((1 - (1 - \mu_2)^\beta)(1 - \mu_1)^\beta + \beta + (1 - \mu_2)^\beta - 1 \right)}{\left[(1 - \mu_1)(1 - \mu_2) \right]^{1-\beta} \left([(1 - \mu_2)^\beta - 1](1 - \mu_1)^\beta - (1 - \mu_2)^\beta \right)^2}$$

The Joe copula is similar to the Gumbel copula, which can only capture upper tail dependency. The upper tail of the Joe copula is $\lambda_U = 2 - 2^{1/\beta}$ for all β larger or equal to one.

One of the limitations of the Clayton, Gumbel, and Joe copulas is that they can only measure positive dependence but not negative dependence. However, in financial data negative dependencies occur between variables. To overcome this limitation, we rotate the Clayton, Gumbel, and Joe copulas for 90° , 180° , and 270° . A more detailed explanation of rotated copulas can be found in [Sriboonchitta et al. \(2013\)](#).

A copula can be rotated 180° (also known as a survival copula) using the following equations:

$$C^{--}(\mu_1, \mu_2) = \mu_1 + \mu_2 - 1 + C(1 - \mu_1, 1 - \mu_2)$$

$$c^{--}(\mu_1, \mu_2) = c(1 - \mu_1, 1 - \mu_2)$$

The 90° rotated copula and its density can be expressed as:

$$C^{-+}(\mu_1, \mu_2) = \mu_1 - C(1 - \mu_1, \mu_2)$$

$$c^{-+}(\mu_1, \mu_2) = c(1 - \mu_1, \mu_2)$$

Finally, the 270° rotated copula and its density can be written as:

$$C^{+-}(\mu_1, \mu_2) = \mu_1 - C(\mu_1, 1 - \mu_2)$$

$$c^{+-}(\mu_1, \mu_2) = c(\mu_1, 1 - \mu_2)$$

The static copula models as presented above cannot capture the dynamic dependence structure among

variables. However, [Lu et al. \(2014\)](#) show that the performance of time-varying copulas is always superior to that of static copulas. [Patton \(2006\)](#) proposes a time-varying copula model by allowing the parameter to evolve over time using transformations of the lagged data and an autoregressive term. This method is also known as the autoregressive moving average (ARMA) process. Nonetheless, as mentioned earlier, the Gumbel, Clayton, and Joe copulas from the Archimedean family can reflect only positive dependence and not negative dependence, namely, the range of Kendall's Tau for these Archimedean copulas is in $[0, 1]$. The ARMA process proposed by [Patton \(2006\)](#) cannot capture negative dependence and is not realistic for our purpose of constructing a FSI. In order to capture both time-varying positive and negative dependence structures, we apply the window rolling method and propose a novel algorithm (1) as shown below, such that the time-varying Kendall's Tau series from the Gumbel, Clayton, and Joe copulas can take values in the range of $[-1, 1]$.

Algorithm 1: Time-varying copula

Result: To obtain Kendall's Tau with a range of $[-1, 1]$

1. Set a 500 day-long rolling window for the two selected variables (μ_1, μ_2) ;
 2. Fit the data into the selected copulas (Gumbel, Clayton, and Joe), and rotate the copulas 90° , 180° , and 270° ;
 3. The best model is selected from the copulas and the rotated copulas based on Akaike information criterion(AIC);
 4. The parameter obtained from the best fitted copula is converted into Kendall's Tau;
 5. Repeat steps 1 to 4 until a series of Kendall's Tau is obtained;
-

4. Copula results

4.1. Static copula

The estimation results of static copula models including the corresponding Kendall's Tau coefficients are presented in [Table 2](#). For the Clayton, Gumbel, and Joe copulas, the 90° , 180° , and 270° rotations are applied to model the negative dependency of the sectors. The best models for each copula are selected based on lowest AIC, and these are underlined in the table. All the copula models show that the dependence of the banking-security sector is negative except for the Joe copula. However, the dependence of the banking-forex sector is found to be weak and positive in all copula models except for the Frank copula. The dependence structure of the security-forex sector is positive and stronger compared to the other sectors. According to

Table 2: Static copula

		bank-sec	bank-fx	sec-fx		bank-sec	bank-fx	sec-fx	
Gaussian	Φ	-0.119*** (0.014)	0.031** (0.014)	0.364*** (0.011)	Frank	θ	-1.149*** (0.084)	-0.330*** (0.084)	1.942*** (0.087)
	τ	-0.076	0.020	0.237		τ	-0.125	-0.036	0.203
	AIC	-72.181	-2.923	-735.309		AIC	-184.441	-13.567	-498.520
Student's t	T	-0.158*** (0.015)	0.011 (0.017)	0.339*** (0.014)					
	v	11.229*** (1.676)	30.000	8.109 (1.384)					
	τ	-0.101	0.007	0.220					
	AIC	-126.234	-5.268	-771.311					
Clayton	α	0.000 (0.023)	0.027** (0.014)	0.313*** (0.020)	<i>R180</i>	α	0.065*** (0.012)	0.059*** (0.013)	0.593*** (0.023)
	τ	0.000	0.013	0.135		τ	0.031	0.029	0.229
	AIC	2.344	-2.123	-312.520		AIC	-30.966	<u>-22.047</u>	<u>-969.866</u>
<i>R90</i>	α	-0.106*** (0.020)	-0.053 (0.035)	-0.000 (0.032)	<i>R270</i>	α	-0.145*** (0.017)	-0.000 (0.015)	-0.000 (0.020)
	τ	-0.050	-0.026	0.000		τ	-0.068	0.000	0.000
	AIC	-32.842	-8.188	2.358		AIC	<u>-64.271</u>	2.189	2.438
Gumbel	δ	1.019*** (0.005)	1.026*** (0.006)	1.305*** (0.013)	<i>R180</i>	δ	1.000*** (0.010)	1.000*** (0.008)	1.228*** (0.013)
	τ	0.018	0.026	0.234		τ	0.000	0.000	0.185
	AIC	-24.519	<u>-25.833</u>	<u>-986.554</u>		AIC	2.590	2.029	-459.051
	<i>R90</i>	δ	-1.090*** (0.011)	-1.000*** (0.009)		-1.000*** (0.013)	<i>R270</i>	δ	-1.061*** (0.011)
τ		-0.083	0.000	0.000	τ	-0.058		0.000	0.000
AIC		<u>-80.483</u>	2.216	2.858	AIC	-30.211		2.003	2.776
Joe	β	1.057*** (0.009)	1.042*** (0.008)	1.461*** (0.021)	<i>R180</i>	β	1.000*** (0.014)	1.000*** (0.011)	1.218*** (0.017)
	τ	0.032	0.024	0.206		τ	0.000	0.000	0.111
	AIC	-75.223	-38.726	-1002.975		AIC	2.465	2.032	-220.423
	<i>R90</i>	β	-1.104*** (0.015)	-1.000*** (0.014)		-1.000*** (0.018)	<i>R270</i>	β	-1.015*** (0.017)
τ		-0.057	0.000	0.000	τ	-0.009		0.000	0.000
AIC		-46.194	2.243	2.516	AIC	1.226		2.003	2.421

Notes: Standard errors in parentheses. *, **, and *** denote significance at the 10, 5, and 1% level. R90, R180, and R270 stand for the rotated 90°, 180°, and 270° models, respectively. The underlined value is the lowest AIC among the copula and rotated copula. The bold value is the best copula selected among the copula model base on the lowest AIC. Bank, sec, and fx represent the banking, security, and forex sectors, respectively.

Table 3: Tail dependency

Copula	Banking-Security		Banking-Forex		Security-Forex	
	Lower	Upper	Lower	Upper	Lower	Upper
Student's t	1.4186×10^{-3}	1.4186×10^{-3}	5.0300×10^{-6}	5.0300×10^{-6}	6.2658×10^{-2}	6.2658×10^{-2}
Clayton	0.0000	0	6.1300×10^{-12}	0	1.0895×10^{-1}	0
Clayton R180	0	2.1800×10^{-5}	0	7.6700×10^{-6}	0	3.1098×10^{-1}
Gumbel	0	2.5047×10^{-2}	0	3.5174×10^{-2}	0	2.9900×10^{-1}
Gumbel R180	2.3416×10^{-4}	0	2.3416×10^{-4}	0	2.4112×10^{-1}	0
Joe	0	7.3367×10^{-2}	0	5.5541×10^{-2}	0	3.9265×10^{-1}
Joe R180	2.3416×10^{-4}	0	2.3416×10^{-4}	0	2.3320×10^{-1}	0
Average	4.7174×10^{-4}	2.4964×10^{-2}	1.1834×10^{-4}	2.2682×10^{-2}	1.6148×10^{-1}	2.6632×10^{-1}

Notes: The average is calculated by adding all the tail coefficients and dividing by four.

AIC, the Joe copula is the best model among all the selected copulas to fit the joint distribution for the banking-forex sector and the security-forex sector. However, the Frank copula outperforms the Joe copula for fitting the dependence structure of the banking-security sector. The best fitted copula model is written in bold on the values of AIC in the table.

Table 3 presents the lower and upper tail dependencies for the copula models.² The lower tail dependence can be interpreted as the probability of both sectors experiencing low financial stress. On the other hand, the upper tail shows the probability of high financial stress occurring between the two selected markets. From Table 3, the Student's t copula shows that the extreme joint probability is the highest for the security-forex pair (6.2658×10^{-2}), followed by banking-security pair (1.4186×10^{-3}) and the banking-forex pair (5.0300×10^{-6}). From the Student's t copula result, the dependence structure of the security-forex pair entails the heaviest tails followed by the banking-security and banking-forex pairs. The averages for the lower and upper tails of each of the copulas are presented in the table. In general, it is clear that the upper tail tends to be higher compared to the lower tail. This can be interpreted insofar as the dependence structure is skewed to the right as they are more correlated during periods of high financial stress. Furthermore, both the lower and upper tail dependencies for the security-forex pair are the highest, which is consistent with

²There is no tail dependency for the Gaussian and Frank copulas.

Table 4: Average AIC for time-varying copula

Copula	banking-security	banking-forex	security-forex
Gaussian	-113.6041	-93.3907	-196.6471
Student t	-112.8537	-94.7397	-198.7838
Clayton	-157.2472	-127.5121	-218.7487
Gumbel	-129.1592	-107.2263	-213.0850
Frank	-104.5676	-92.5832	-172.3549
Joe	-157.8356	-127.3517	-217.2937

Notes: The bold value is the best fitted copula model base on the lowest AIC.

the Student’s t copula finding.

4.2. Time-varying copula

As mentioned in the previous section, a static copula cannot reflect the dynamic behavior of the dependence structures of market-specific stress. Therefore, we apply a 500 day-long rolling window time-varying copula with the algorithm (1) to model the dependence structures among the subindices.³ The best model is selected based on the average AIC as presented in Table 4. The Joe copula is the best fitted for the dependence structure of the banking-security pair, and the Clayton copula is the best fitted for the banking-forex and security-forex pairs. Kendall’s Tau coefficients from the selected model are presented in Figure 3.

5. Country-level FSSI

5.1. Aggregation of FSSI

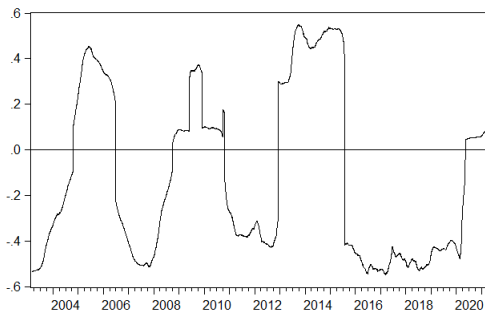
The aggregation of individual stress indices is an important aspect of constructing the FSSI (Illing and Liu 2006). As shown in Section 2.3, we adopt a portfolio theory-based approach to building the FSSI. The first step of construction is to develop sub-component index for each sector (I_{BK}, I_{SC}, I_{FX}). The plots of three sub-component indices are presented in Figure 1.

The next step is to aggregate the subindices based on the portfolio theory approach as stated in Equation 1 using time-varying correlations C_t estimated by the best fitted copula model in Section 4. Figure 4 provides an overview of the FSSI with selected major financial stress events¹.

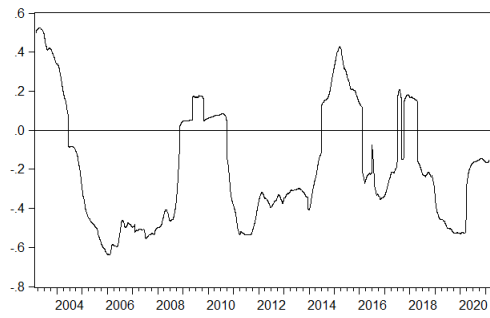
As seen from the figure, the systemic financial risk increases during the notably adverse financial events. The surge is most pronounced in the 2008 GFC, 2011 Black Monday stock crash and 2020 COVID-19 crisis periods. In March 2020 as COVID-19 pandemic spread globally and governments around the world

³As a robustness check, we also apply a 400 and 600 day-long rolling window. Detailed results are available upon request.

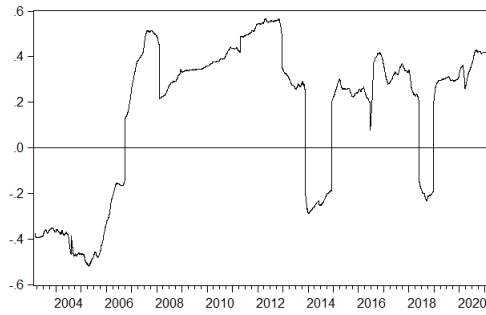
¹The selection of major financial stress events is based on Craig (2020) and authors’ consideration



(a) banking-security



(b) banking-forex



(c) security-forex

Figure 3: Time-varying Kendall's Tau

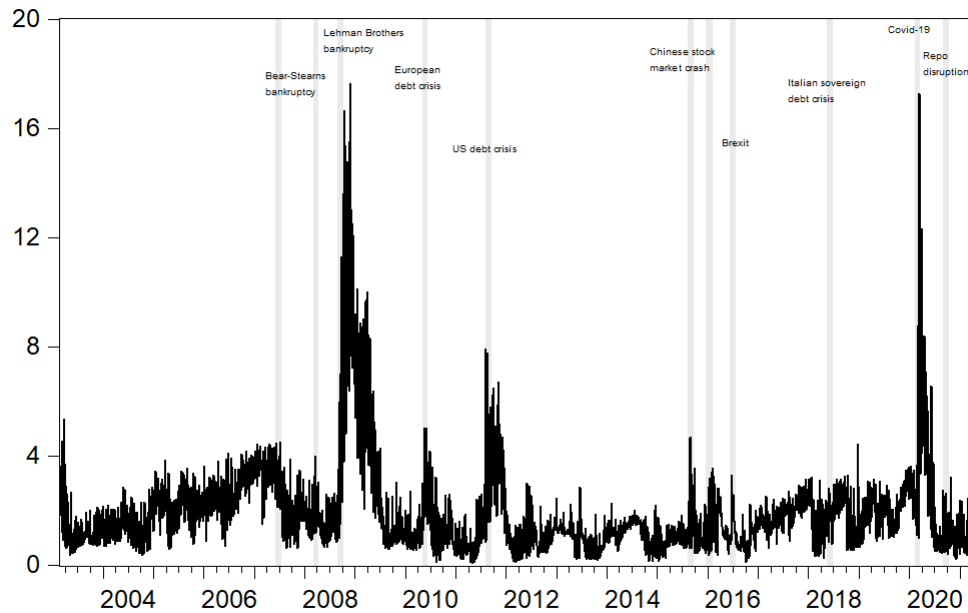


Figure 4: Financial systemic stress index

shutdown nonessential business activities, mounting economic uncertainty led to a peak in financial stress, in which the intensity echoed that of 2008 GFC. However, the duration of systemic stress during the COVID-19 period is shorter than the GFC counterpart, reflecting swift rebounds in financial markets in tandem with the stronger-than-expected recovery of the global economy.

5.2. Identifying systemic financial risk

Using the FSSI constructed in the previous section, we can identify the states of systemic financial risk in the US financial system. In the existing literature, there are three commonly used methods to identify financial stress episodes. The approach of the Bank of Canada (see [Illing and Liu \(2006\)](#)) and IMF is to classify financial stress as severe when the index exceeds the historical mean by one or two standard deviations. The disadvantage of this approach is that the choice of threshold is arbitrary, and the number of standard deviations by which the index exceeds the mean can change drastically with the presence of extreme observations. A second way of identification is to classify the FSSI as a risk episode whenever it equals or exceeds the value of the index in some benchmark crisis episodes, such as 1989 Black Monday or 2008 GFC. This approach is adopted in [Hakkio et al. \(2009\)](#). The final approach is to use the Markov-Switching model to identify different systemic financial risk states. In this paper, we followed the latter approach and built a Markov Switching Autoregressive (MS-AR) model to conduct the systemic risk episode identification.

Table 5: MS-AR models with different fitness criterion

	Log likelihood	AIC	BIC	HQ
MS-AR(1)	-5901.280	2.514	2.522	2.517
MS-AR(2)	-5364.898	2.286	2.296	2.290
MS-AR(3)	-5881.618	2.507	2.518	2.511
MS-AR(4)	-5104.753	2.177	2.190	2.182
MS-AR(5)	-5033.547	2.148	2.162	2.153
MS-AR(6)	-5022.373*	2.144*	2.159*	2.149*

Notes: AIC, BIC and HQ represent Akaike information criterion, Bayesian information criterion and Hannan Quinn respectively. * indicate that the best model selected based on highest log likelihood and lowest AIC, BIC and HQ.

To fit the FSSI data in the MS-AR model, we test the unit root of the series using the ADF approach. The T-statistic of the test is -4.753 and the p-value is 0.0001, implying the FSSI is stationary at 1% significant level. To find the best two-regime MS-AR model, we estimate six models with number of lag from 1 to 6. The estimation results with fitness criterion are shown in Table 5. According to the fitness criterion, MS-AR(6) is the best among six models. Hence, we adopt MS-AR(6) in the following identification. In the two-regime Markov-switching model, we set the low systemic risk state as 1 and high systemic risk state as 2. The MS-AR(6) model for the FSSI can be expressed as:

$$FSSI_t = \begin{cases} c_1 + \sum_{i=1}^6 \alpha_{1,i} FSSI_{t-i} + \varepsilon_{1,t} & \text{if } s_t = 1 \\ c_2 + \sum_{i=1}^6 \alpha_{2,i} FSSI_{t-i} + \varepsilon_{2,t} & \text{if } s_t = 2 \end{cases} \quad (8)$$

where $\varepsilon_{1,t}$ and $\varepsilon_{2,t}$ are i.i.d and s_t is unobservable variable. The probability of switching between State 1 and State 2 follows the first order Markov chain. The transition matrix can be written as:

$$\mathbf{P} = \begin{bmatrix} P(s_t = 1|s_{t-1} = 1) & P(s_t = 1|s_{t-1} = 2) \\ P(s_t = 2|s_{t-1} = 1) & P(s_t = 2|s_{t-1} = 2) \end{bmatrix} = \begin{bmatrix} P_{11} & P_{12} \\ P_{21} & P_{22} \end{bmatrix} \quad (9)$$

The estimation results of transition matrix are shown in Table 6. $P_{11} = 0.9863$ means that the probability of the US financial stress staying at a low level is 0.9863. In other words, the low stress state is stable and hardly transits to a high stress state. Meanwhile, the probability of a high stress state is 0.3360 and it is relatively easy to transit to a low stress state with a probability of 0.6640. The expected duration for low stress and high stress is 72.9055 and 1.5060, respectively. This finding implies that systemic financial risk in the US is low for most periods of the sample, and high systemic risk only occurs for a few periods.

We further plot the regime probabilities in Figure 5. Generally, the high stress periods are shorter than

Table 6: Transition matrix and state duration

	Transition matrix		Expected duration	
	1	2	1	2
1	0.9863	0.0137	72.9055	1.5060
2	0.6640	0.3360		

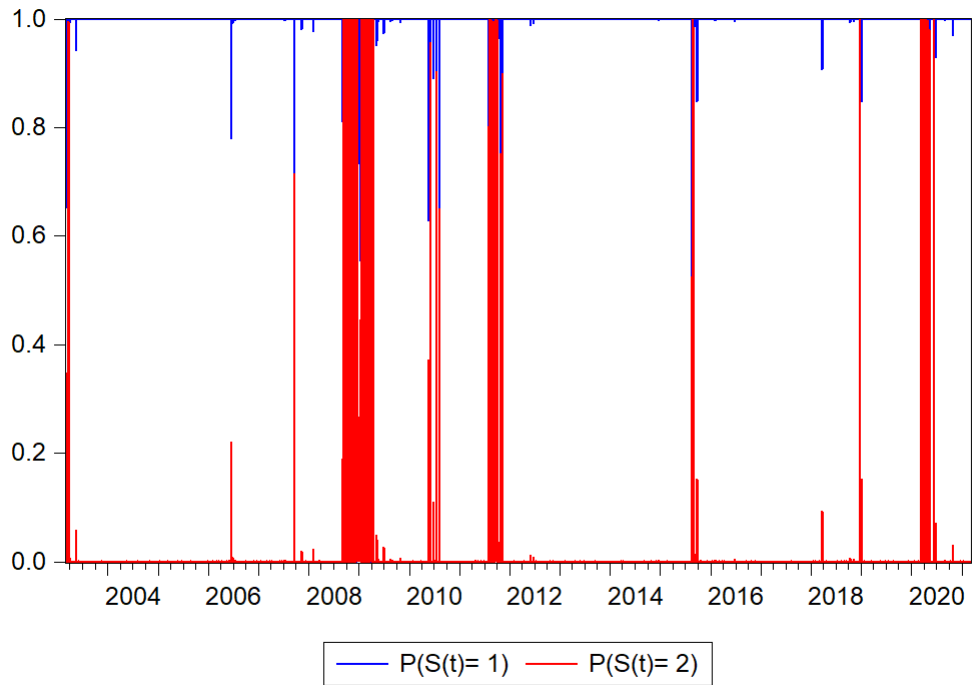


Figure 5: Markov switching smoothed regime probabilities

low stress periods. The high stress periods are clustering at 2008-2009, 2011 and 2020, which are exactly corresponding to the crisis periods highlighted in [Figure 4](#). This shows that the FSSI can be used as a crisis warning indicator. When the FSSI surges and the state is transiting to a high stress regime, the probability of systemic financial crisis increases. Take 2008 GFC as an example: the market state transited from low to high in early 2008, indicating the increase of systemic financial risk in the US. As the financial stress index constructed in this paper is in daily frequency, the index is more volatile during high stress periods. The state transition is also more frequent, which can be considered as another signal of excessive systemic financial risk.

6. Conclusion

This work proposes a reproducible approach to measuring and monitoring financial stress, thus having important implications for the macroprudential regulation of the financial system. This is especially pertinent given the surge in financial frailty during the ongoing COVID-19 crisis. We combined the portfolio-theory based approach proposed by [Hollo et al. \(2012\)](#) and the copula method, which offers a flexible method for modeling nonlinear dependence structures across financial sectors. This way, our composite indicator for financial stress can capture the systemic nature of a crisis, which is not adequately represented by the linear correlation measures, and reduce the chance of underestimating financial risk in the presence of asymmetric dependence between financial segments.

We find that the dependence structures between the market-specific stresses are best explained by Archimedean copula families. Specifically, in the dynamic setting, the Joe and Clayton copulas are the best models based on AIC, signaling the presence of asymmetric tail dependencies between individual market stresses over time.

Using Kendall's Tau coefficients from the best fitted time-varying copulas, the market specific stresses are aggregated to a single FSSI. We apply our MS-AR model to identify different states of systemic financial risk based on the FSSI. We find that most of the sample periods constitute low stress episodes and a few periods can be classified as high stress states. The Markov state identification result, based on FSSI data, is able to detect several recent instances of financial turbulence in the US and confirms that the FSSI is a reliable indicator for measuring systemic financial risk.

Our construction method for the country-specific FSSI can be considered the first step towards a more in-depth analysis of financial instability. For instance, the copula method can be used to measure the systemic

stress experienced by regional and global financial systems. We may also apply the FSSIs of a wide range of markets to study various important topics in international finance, such as financial stress spillovers across regions, and linkages between the FSSIs and other economic and financial indicators.

References

- Aboura, S. and B. van Roye (2017). Financial stress and economic dynamics: The case of France. *International Economics* 149, 57–73.
- Albulescu, C. T., A. K. Tiwari, and Q. Ji (2020). Copula-based local dependence among energy, agriculture and metal commodities markets. *Energy* 202, 117762.
- Aloui, R., S. Hammoudeh, and D. K. Nguyen (2013). A time-varying copula approach to oil and stock market dependence: The case of transition economies. *Energy Economics* 39, 208–221.
- Apostolakis, G. and A. P. Papadopoulos (2014). Financial stress spillovers in advanced economies. *Journal of International Financial Markets, Institutions and Money* 32, 128–149.
- Balakrishnan, R., S. Danninger, S. Elekdag, and I. Tytell (2011). The transmission of financial stress from advanced to emerging economies. *Emerging Markets Finance and Trade* 47(sup2), 40–68.
- Bouri, E., R. Gupta, C. K. M. Lau, D. Roubaud, and S. Wang (2018). Bitcoin and global financial stress: A copula-based approach to dependence and causality in the quantiles. *The Quarterly Review of Economics and Finance* 69, 297–307.
- Cardarelli, R., S. Elekdag, and S. Lall (2011). Financial stress and economic contractions. *Journal of Financial Stability* 7(2), 78–97.
- Cevik, E. I., S. Dibooglu, and T. Kenc (2013). Measuring financial stress in Turkey. *Journal of Policy Modeling* 35(2), 370–383.
- Chau, F. and R. Deesomsak (2014). Does linkage fuel the fire? The transmission of financial stress across the markets. *International Review of Financial Analysis* 36, 57–70.
- Craig, B. R. (2020). How well does the Cleveland Fed’s systemic risk indicator predict stress? *Economic Commentary* (EC 2020-28).
- Das, D., S. B. Kumar, A. K. Tiwari, M. Shahbaz, and H. M. Hasim (2018). On the relationship of gold, crude oil, stocks with financial stress: A causality-in-quantiles approach. *Finance Research Letters* 27, 169–174.

- Duprey, T., B. Klaus, and T. Peltonen (2017). Dating systemic financial stress episodes in the EU countries. *Journal of Financial Stability* 32, 30–56.
- Elsayed, A. H. and L. Yarovaya (2019). Financial stress dynamics in the MENA region: Evidence from the Arab Spring. *Journal of International Financial Markets, Institutions and Money* 62, 20–34.
- Fisher, N. and P. Switzer (1985). Chi-plots for assessing dependence. *Biometrika* 72(2), 253–265.
- Fisher, N. and P. Switzer (2001). Graphical assessment of dependence: Is a picture worth 100 tests? *The American Statistician* 55(3), 233–239.
- Hakkio, C. S., W. R. Keeton, et al. (2009). Financial stress: what is it, how can it be measured, and why does it matter? *Economic Review* 94(2), 5–50.
- Hollo, D., M. Kremer, and M. Lo Duca (2012). CISS-a composite indicator of systemic stress in the financial system.
- Hubrich, K. and R. J. Tetlow (2015). Financial stress and economic dynamics: The transmission of crises. *Journal of Monetary Economics* 70, 100–115.
- Illing, M. and Y. Liu (2006). Measuring financial stress in a developed country: An application to Canada. *Journal of Financial Stability* 2(3), 243–265.
- Kliesen, K. L., D. C. Smith, et al. (2010). Measuring financial market stress. *Economic Synopses*.
- Louzis, D. P. and A. T. Vouldis (2012). A methodology for constructing a financial systemic stress index: An application to Greece. *Economic Modelling* 29(4), 1228–1241.
- Lu, X. F., K. K. Lai, and L. Liang (2014). Portfolio value-at-risk estimation in energy futures markets with time-varying copula-GARCH model. *Annals of Operations Research* 219(1), 333–357.
- MacDonald, R., V. Sogiakas, and A. Tsopanakis (2018). Volatility co-movements and spillover effects within the Eurozone economies: A multivariate GARCH approach using the financial stress index. *Journal of International Financial Markets, Institutions and Money* 52, 17–36.
- Melvin, M. and M. P. Taylor (2009). The crisis in the foreign exchange market. *Journal of International Money and Finance* 28(8), 1317–1330.

- Nelson, W. R. and R. Perli (2007). Selected indicators of financial stability. *Risk Measurement and Systemic Risk* 4, 343–372.
- Nikoloulopoulos, A. K., H. Joe, and H. Li (2012). Vine copulas with asymmetric tail dependence and applications to financial return data. *Computational Statistics & Data Analysis* 56(11), 3659–3673.
- Oet, M. V., J. M. Dooley, and S. J. Ong (2015). The financial stress index: Identification of systemic risk conditions. *Risks* 3(3), 420–444.
- Park, C.-Y. and R. V. Mercado Jr (2014). Determinants of financial stress in emerging market economies. *Journal of Banking & Finance* 45, 199–224.
- Patton, A. J. (2006). Modelling asymmetric exchange rate dependence. *International Economic Review* 47(2), 527–556.
- Sklar, M. (1959). Fonctions de repartition an dimensions et leurs marges. *Publ. Inst. Statist* 8, 229–231.
- Sriboonchitta, S., H. T. Nguyen, A. Wiboonpongse, and J. Liu (2013). Modeling volatility and dependency of agricultural price and production indices of Thailand: Static versus time-varying copulas. *International Journal of Approximate Reasoning* 54(6), 793–808.
- Tsay, R. S. (2013). *Multivariate time series analysis: with R and financial applications*. John Wiley & Sons.
- Yeap, X. W., H. H. Lean, M. G. Sampid, and H. M. Hasim (2020). The dependence structure and portfolio risk of Malaysia’s foreign exchange rates: the Bayesian GARCH–EVT–copula model. *International Journal of Emerging Markets*.
- Zhang, D., M. Yan, and A. Tsopanakis (2018). Financial stress relationships among Euro area countries: an R-vine copula approach. *The European Journal of Finance* 24(17), 1587–1608.